Physica E 139 (2022) 115188

Contents lists available at ScienceDirect

Physica E: Low-dimensional Systems and Nanostructures

journal homepage: www.elsevier.com/locate/physe

Investigation of NH_3 adsorption on noble metal modified $MoSe_2$

Ahmad I. Ayesh

Physics Program, Department of Mathematics, Statistics and Physics, College of Arts And Sciences, Qatar University, P. O. Box 2713, Doha, Qatar

ARTICLE INFO

Keywords:
$MoSe_2$
NH_3
First principles
DFT
Pt
Au
Ag

ABSTRACT

Gas pollutants represent hazard for the quality of the ambient environment, thus, the development of sensitive and selective gas sensors is essential to monitor and maintain its decent quality. The adsorption of NH_3 gas on pristine and noble metal doped molybdenum diselenide ($MoSe_2$) structures is investigated by density functional theory (DFT) computations. The metals used for doping are Pt, Au, Ag, and their combination. The work discusses the effect of doping on the adsorption energy, charge transferred among $MoSe_2$ structures and NH_3 gas, adsorption distance, density of states (DOS), and band structure. The DOS as well as band structure of the modified $MoSe_2$ show substantial modifications in the electronic properties as compared with the pristine structure. New energy bands are developed close to the Fermi level due to doping of $MoSe_2$ structure. The NH_3 gas adsorption on the doped structures is significantly enhanced, compared with the pure $MoSe_2$ structure, where the adsorption energy and distance for NH_3 gas are improved, thus, the sensitivity is enhanced sensitivity compared with the pure $MoSe_2$ structure. This investigation demonstrates that noble metal doping of $MoSe_2$ can be an effective method to develop sensitive detectors for NH_3 gas.

1. Introduction

The expansion of industrial activities of human is associated with escalation of emissions of hazardous gases, for example: CO, CO_2, NO, NO_2, and NH_3 [1,2]. Ammonia (NH_3) is a highly harmful gas to the environment and human health, and it is a common chemical utilized and generated by various agricultural and industrial activates [3]. The human exposure limit should be less than 50 ppm for safe work environment [4], while the indoor long-term exposure limit is 25 ppm. Long term exposure to NH_3 beyond those limits causes serious impact on the respiratory system along with eyes irritation, severe burns, and injuries [5]. Therefore, sensitive and selective detection of ammonia is essential in various sectors including ammonia production plants, agricultural fertilizer industry, and units of food processing.

Two dimensional (2D) transition metals are distinguished with their extraordinary characteristics which may be utilized in various fields of applications [6,7]. For example, they are used intensively for gas and chemical sensor applications due to their high reactivity that is assigned to the large number of reactive cites generated by the large surface area [8–10]. Molybdenum diselenide ($MoSe_2$) monolayer is a semiconducting dichalcogenides 2D material with superior electrical and structural properties that make it ideal for multiple applications including gas sensors [11]. $MoSe_2$ 2D structure consists of two layers (upper and lower) of Se atoms and a layer of Mo atoms that is sandwiched between them. Covalent bonds are established between one Mo atom and six Se atoms [12,13]. The 2D structure of $MoSe_2$ has a direct bandgap ($E_g \cong 1.6\ V$), dissimilar to the bulk $MoSe_2$ that has an indirect bandgap [14]. Moreover, $MoSe_2$ exhibits extraordinary catalytic activity because of its high surface area, and its electrical conductivity is stimulated by the electrocatalytically unsaturated active Se atoms at the edges [15]. Therefore, $MoSe_2$ is considered an attractive system for multiple applications including gas sensing.

Recent research groups focused recently on investigating the utilization of $MoSe_2$ for multiple applications including chemical and gas sensors, catalysis, energy storage, and optoelectronics [16,17]. For instance, $MoSe_2$ was investigate for utilization to produce battery electrodes where it was modified to reduced its conductivity with an objective of boosting its efficiency [18]. The effect of doping $MoSe_2$ by Nb and its impact on the sensitivity against NO_2 gas was investigated by S. Choi et al. [19]. The doping was realized by a plasma deposition method, and the doped structure with low Nb concentrations demonstrated enhanced sensitivity against of NO_2 gas. $MoSe_2$ was investigated experimentally for its sensitivity for NH_3, and the results reveal enhancement of its response upon composition with Au [20]. This enhancement was assigned to the rather stable and small grain boundaries. Density functional theory (DFT) computations as well as experimental investigation were conducted by D. Zhang et al. to examine the NH_3 gas sensing behavior of $MoSe_2$ nanoflower consequent to its doping

E-mail address: ayesh@qu.edu.qa.

https://doi.org/10.1016/j.physe.2022.115188
Received 17 September 2021; Received in revised form 18 January 2022; Accepted 1 February 2022
Available online 4 February 2022

with Pd [16]. They reported considerable enhancement of the sensitivity against NH_3 gas. Furthermore, H. Luo et al. investigated the adsorption of NH_3 and NO_2 gases on $MoSe_2$ doped with Al, Si, and P atoms using DFT computations [21]. They demonstrated that the doped structures exhibit enhanced adsorption as compared with the pristine $MoSe_2$ structure. Furthermore, doping increases the influence of orbital hybridization among the gas molecules and $MoSe_2$, and stimulate charge transfer.

The adsorption parameters of NH_3 gas on pristine and noble metal doped $MoSe_2$ structures are examined using the computational first principles - DFT in this work. The noble metal used for doping are: Pt, Au, Ag, and their combination. The influence of doping on density of states, band structure, bandgap energy, NH_3 adsorption energy as well as distance, along with the charge transferred among a structure and NH_3 are investigated. This report illustrates that the noble metal doping of $MoSe_2$ introduces substantial modifications of its electronic characteristics. Besides, doping of $MoSe_2$ structure boosts its adsorption of NH_3 gas.

2. Computational method

The adsorption of NH_3 gas on pristine and modified $MoSe_2$ atomic structures was explored using first principles - DFT [22,23]. A software package for atomistic quantum simulation (ATK) from Synopsys was used to compute the electronic characteristics, gas adsorption parameters, and band structure [22,24–26]. A supercell of $MoSe_2$ monolayer of 5×5 was assembled and doped with Pt, Au, Ag, and their combination. The doped structures were named as: Pt–$MoSe_2$, Au–$MoSe_2$, Ag–$MoSe_2$, and Pt–Au–Ag–$MoSe_2$. The modification was achieved through substitution of a central Se atom by Pt, Au, or Ag. For the co-doping, three central Se atoms were replaced by Pt, Au, and Ag. The exchange correlation density-functional of Perdew–Burke–Ernzerh (PBE) was included within the approximations of generalized gradient (GGA) to describe electron correlation and exchange [27,28]. The influence of van der Waals force was corrected by employing the Grimme function (DFT-D2) [28]. The optimization was established using a cutoff energy mesh of 100 Hartree at a temperature of 300 K. The maximum tolerances of stress and force during optimization were 0.1 GPa and 0.01 eV/Å. The Monkhorst-Pack (MP) grid was utilized to choose the k-point sampling for Brillouin-zone of $4 \times 4 \times 1$, and it was applied for all geometry optimizations and computations of electronic characteristics [29].

The energy of NH_3 gas adsorption ($E_{Ad.}$) on pristine or modified $MoSe_2$ structures was evaluated using the equation [30–32]:

$$E_{Ad.} = E_{MoSe_2+NH_3} - (E_{MoSe_2} + E_{NH_3}) \quad (1)$$

where $E_{MoSe_2+NH_3}$ denotes the total energy of either a pristine or modified $MoSe_2$ structure with an adsorbed NH_3 gas molecule. E_{MoSe_2} denotes the total energy of either a pristine or modified $MoSe_2$ structure. E_{NH_3} denotes the total energy of NH_3 gas molecule. The charge transferred between NH_3 and a pristine or modified $MoSe_2$ structure upon adsorption (Δq) was employed to evaluate the degree of NH_3 adsorption, and it was calculated using the method of Mulliken population [31,33]:

$$\Delta q = q_f - q_i \quad (2)$$

where, q_f and q_i indicate the net Mulliken charge of NH_3 subsequent and before its adsorption. Moreover, the effects of NH_3 adsorption on density of states (DOS), bandgap energy (E_g), and adsorption distance (d) for pristine and modified $MoSe_2$ structures are evaluated in this investigation.

3. Results and discussion

NH_3 gas adsorption on monolayers of pristine and modified $MoSe_2$ structures is examined in this work. Fig. 1 shows the optimized pristine and modified $MoSe_2$ structures: $MoSe_2$, Pt–$MoSe_2$, Au–$MoSe_2$, Ag–$MoSe_2$, and Pt–Au–Ag–$MoSe_2$. The Mo–Se bond length is 2.58 Å for all $MoSe_2$ based structures. Upon doping, the bond lengths of Mo–Pt,

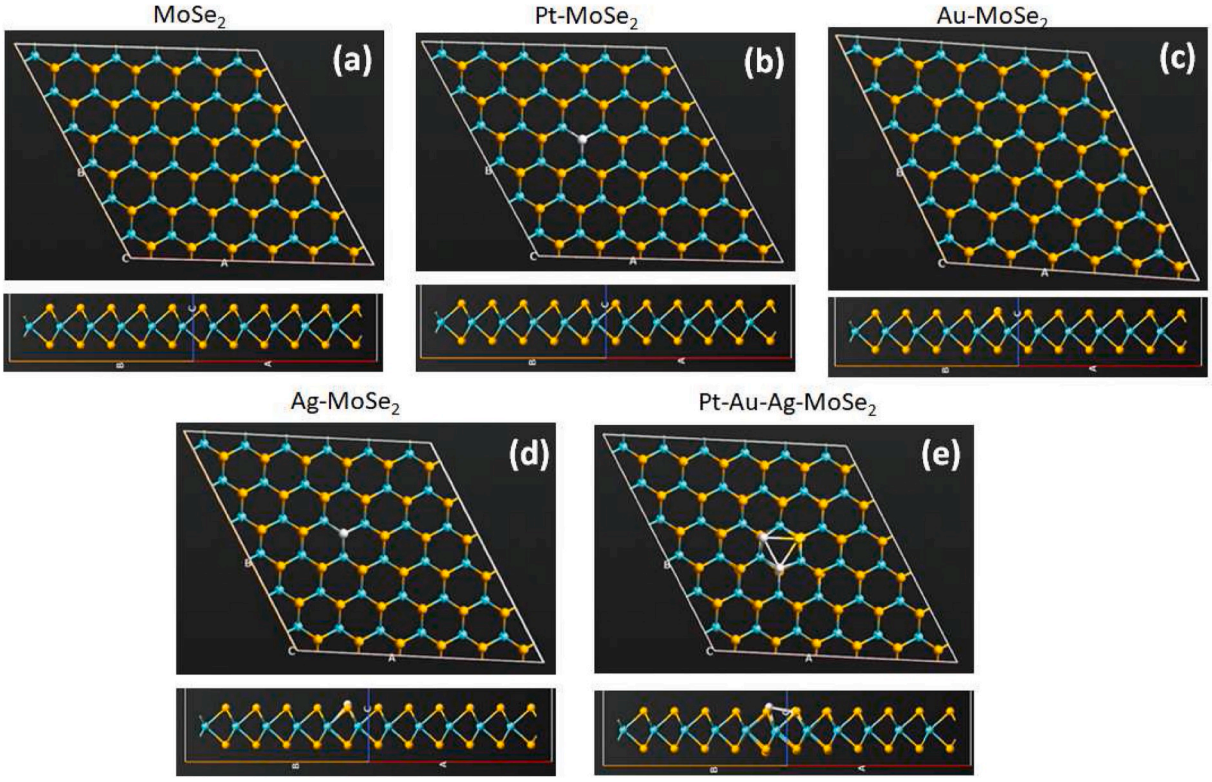

Fig. 1. Top and side views of the optimized pristine and modified $MoSe_2$ structures: a) pristine $MoSe_2$, b) Pt–$MoSe_2$, c) Au–$MoSe_2$, d) Ag–$MoSe_2$, and e) Pt–Au–Ag–$MoSe_2$.

Mo–Au, and Mo–Ag within the mono-doped structures are 2.63, 2.73, and 2.86 Å, respectively. However, the bond lengths of Mo–Pt, Mo–Au, and Mo–Ag for the co-doped structure are 2.77, 2.83, and 2.84 Å, respectively. Doping of a $MoSe_2$ structure modifies its energy levels and thus the band structure. The band structures of the $MoSe_2$, Pt–$MoSe_2$, Au–$MoSe_2$, Ag–$MoSe_2$, and Pt–Au–Ag–$MoSe_2$ monolayers are illustrated in Fig. 2. The figure shows that doping of the $MoSe_2$ structure introduces new energy levels and reduces its bandgap energy. The bandgap energies of the different structures are calculated and presented in Table 1. The table shows that pristine $MoSe_2$ exhibits a direct bandgap with an energy of 1.609 eV which agrees with latest experimental and computational reports [34,35], and indicates that $MoSe_2$ is a semiconducting material. The bandgap energy decreases upon doping due to the introduction of the metal atom(s) within the structure. The minimum value of bandgap energy is for the Ag–$MoSe_2$ structure, while the Pt–$MoSe_2$ and Au–$MoSe_2$ structures exhibit moderate bandgap energies.

The optimized $MoSe_2$, Pt–$MoSe_2$, Au–$MoSe_2$, Ag–$MoSe_2$, and Pt–Au–Ag–$MoSe_2$ structures after adsorption of NH_3 gas molecules are presented in Fig. 3. The figure shows the initiation of chemical bonds (chemisorption) among NH_3 gas molecules and the doped structures. This indicates that both doped and co-doped $MoSe_2$ structures are favorable for NH_3 gas adsorption. No chemical bond appears between NH_3 gas molecule and the pristine $MoSe_2$ structure. The adsorption distance of NH_3 gas molecule on the $MoSe_2$ based structures are presented in Table 2. The table shows that the maximum adsorption distance is for the pristine $MoSe_2$ structure, which agrees with the observation in Fig. 3 where no chemical bond has been developed. On the other hand, the minimum adsorption distance is for the Pt–$MoSe_2$ structure, where a chemisorption is observed as shown in Fig. 3. It should be noted that the adsorption distance for the Au–$MoSe_2$ and Pt–Au–Ag–$MoSe_2$ structures are very close to that of Pt–$MoSe_2$, i.e ~2.3 Å. Fig. 4 shows the band structures of the $MoSe_2$, Pt–$MoSe_2$, Au–$MoSe_2$, Ag–$MoSe_2$, and Pt–Au–Ag–$MoSe_2$ monolayers upon adsorption of NH_3 gas. The figure illustrates noteworthy modifications in the band structures due to adsorption of NH_3, with new sub-bands in both valence and conduction bands. A slight decrease of the bandgap is observed, in general, due to NH_3 gas adsorption. The bandgap values of the structures after modification are presented in Table 2. The appearance of the new sub-bands in Fig. 4 vindicates the variations in the density of states after NH_3 adsorption as discussed below [36].

Table 1
Bandgap of the different $MoSe_2$ based structures.

Structure	$E_g(eV)$
MoSe2	1.609
MoSe2+Pt	1.381
MoSe2–Au	1.244
MoSe2–Ag	0.135
MoSe2+Pt + Au + Au	0.283

Both Fig. 4 and Table 2 show that NH_3 adsorption has been improved because of doping of $MoSe_2$ by either or all of the three metal atoms (Pt, Au, and Ag). The NH_3 gas adsorption energy on pristine as well as doped $MoSe_2$ structures is examined to explore their capacity for applications in the field of gas sensor devices, as presented in Table 2. The table reveals that the noble metal doping of $MoSe_2$ promotes its adsorption energy distinctly. The maximum adsorption energy is for the Au–$MoSe_2$ structure. Nevertheless, the adsorption energy for all the modified $MoSe_2$ structures (by either or all of the three metal elements: Pt, Au, and Ag) is close, i.e $\sim -1\ eV$. The negative value of adsorption energy for NH_3 gas designates its robust adsorption on the modified $MoSe_2$ structures [23], and it indicates that charges have been transferred to NH_3 gas. Table 2 also shows that the maximum charge transferred is for the Pt–$MoSe_2$ structure, although very close value is observed for Au–$MoSe_2$. This is consistent with its maximum adsorption energy and minimum adsorption distance. It should be noted that the negative sign of charge transfer denotes that charges are transferred from NH_3 gas molecule to the $MoSe_2$ based structures.

The best structure for NH_3 gas adsorption is Au–$MoSe_2$ although the $MoSe_2$ structures modified by Pt or all of the three metal elements (Pt, Au, and Ag) exhibit close capacity for NH_3 gas adsorption, i.e $E_{Ad.} \sim 1eV$, $d \sim 2.3$Å, and $\Delta q \sim -0.2e$. The least favorable doped structure for NH_3 gas adsorption is Ag–$MoSe_2$ since it exhibits the maximum adsorption distance of chemisorption. The adsorption energy of NH_3 on Au–$MoSe_2$ structure is 3.5 times greater than that for the pristine $MoSe_2$ structure. Moreover, Fig. 3 of the optimized structures indicates that NH_3 gas

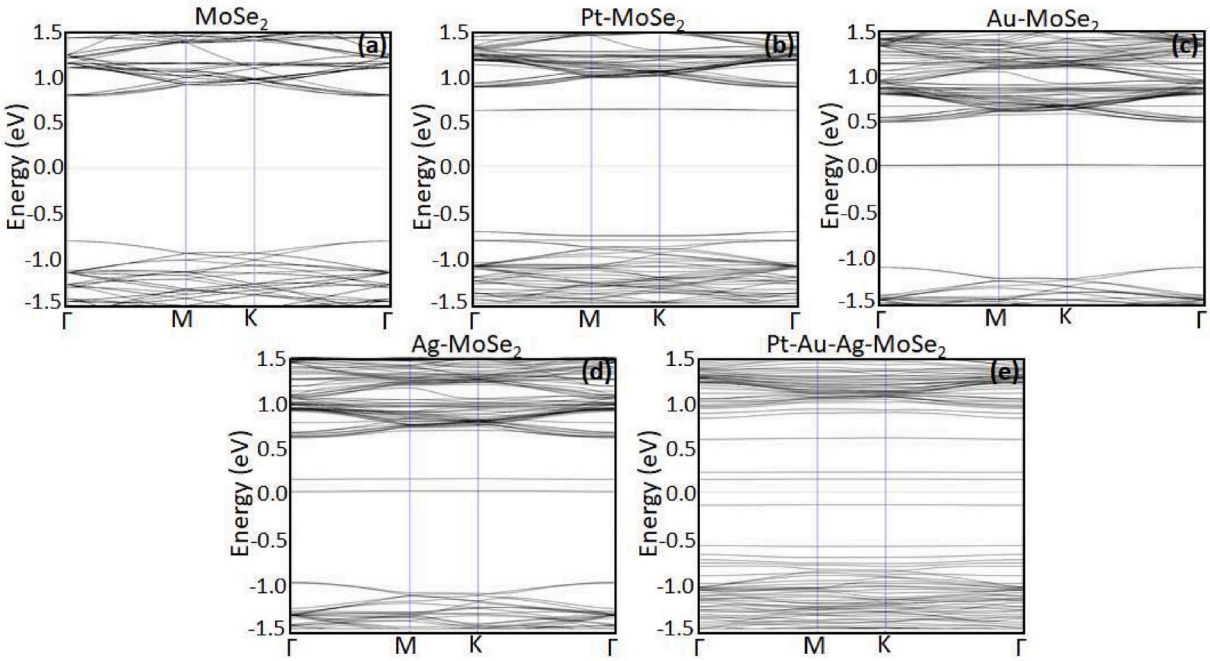

Fig. 2. Band structures of the optimized pristine and modified $MoSe_2$ structures: a) pristine $MoSe_2$, b) Pt–$MoSe_2$, c) Au–$MoSe_2$, d) Ag–$MoSe_2$, and e) Pt–Au–Ag–$MoSe_2$.

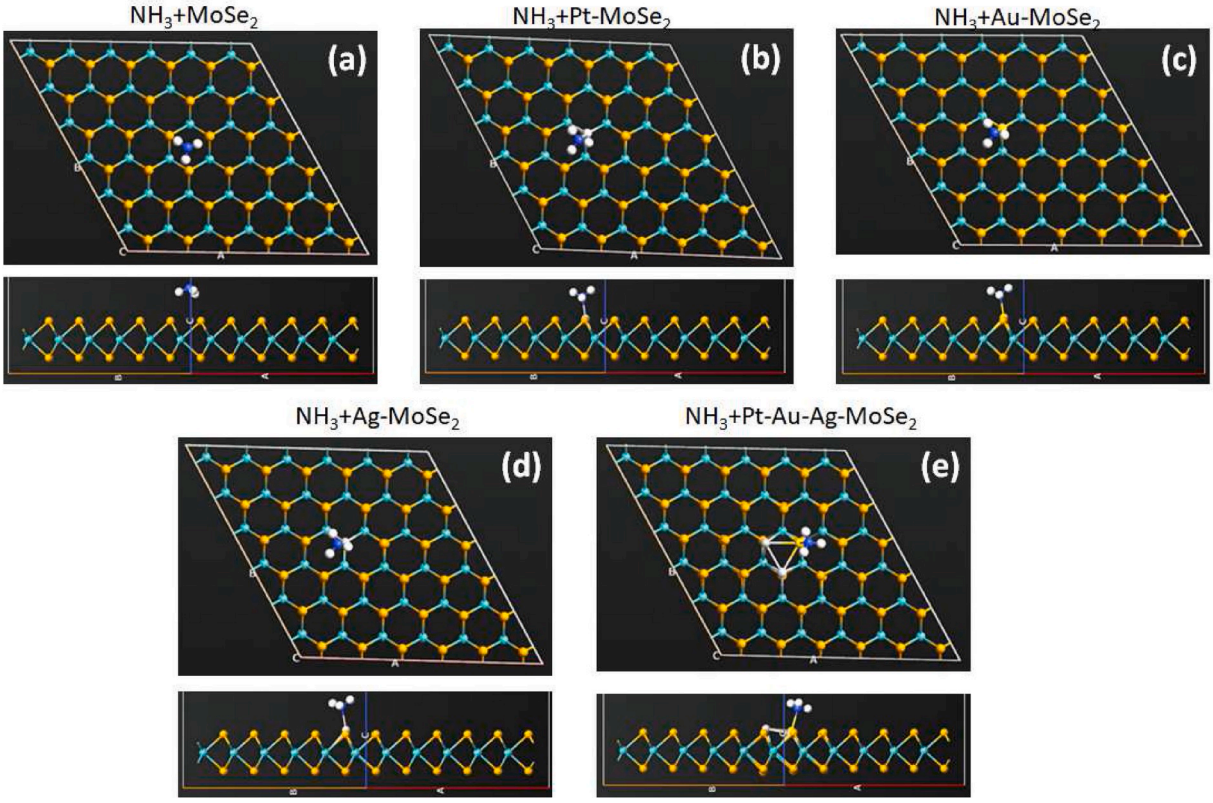

Fig. 3. Top and side views of the optimized pristine and modified $MoSe_2$ structures after adsorption of NH_3 gas: a) pristine $MoSe_2$, b) Pt–$MoSe_2$, c) Au–$MoSe_2$, d) Ag–$MoSe_2$, and e) Pt–Au–Ag–$MoSe_2$.

Table 2
Bandgap, adsorption energy, adsorption distance, charge transferred between NH_3 and the $MoSe_2$ based structures due to gas adsorption.

Structure	$E_g(eV)$	$E_{Ad.}(eV)$	d (Å)	Δq (e)
MoSe2+NH3	1.600	−0.315	2.78	−0.032
MoSe2–Pt–NH3	1.247	−1.057	2.25	−0.219
MoSe2–Au–NH3	0.1474	−1.105	2.27	−0.209
MoSe2–Ag–NH3	0.161	−1.020	2.77	−0.193
MoSe2+Pt + Au + Au + NH3	0.255	−0.954	2.28	−0.204

molecule is chemisorped on the doped $MoSe_2$ structures, however it is physisorped on the pristine $MoSe_2$ structure [37–39]. Accordingly, either of Pt–$MoSe_2$, Au–$MoSe_2$, or Pt–Au–Ag–$MoSe_2$ structures can be utilized efficiently for NH_3 gas sensing applications. It can be concluded that the enhancement of NH_3 gas adsorption is assigned to doping or co-doping with the noble metals. The improvement of gas adsorption due to doping of $MoSe_2$ layer is consistent with recent investigations [16,40]. Noble metal doping alters energy levels for $MoSe_2$ structure and boosts its interaction with NH_3 gas close to the doping site [41].

The effect of NH_3 gas adsorption on DOS of energy levels in the valance and conduction bands for pristine and doped $MoSe_2$ structures is demonstrated in Fig. 5. Fig. 5(a) shows that doping of $MoSe_2$ structure with either or all of the noble metals modifies the DOS of energy levels. Specifically, new bands appear near the Fermi level that justify the variations of the bandgap energy. Clear changes in the intensity of DOS can be observed within the conduction and valance bands, for example at −5.50, −3.73, −2.55, 1.16, 1.52, 1.72, and 2.04 eV. Additionally, new bands are introduced, for example at 4.14 eV. Adsorption of NH_3 gas on pristine $MoSe_2$ structure (Fig. 5(b)) does not cause major variation in the DOS (except minor changes in the intensity at high energy within the conduction band). This is expected since NH_3 gas is physisorped on pristine $MoSe_2$ structure. Clear variations in the intensity of specific energy levels are observed due to NH_3 gas adsorption on the doped $MoSe_2$ structures, as shown in Fig. 5(c) – 5(f). The variations occur at different energy levels, with clear modifications near the Fermi level. For example, changes in the intensity of DOS are observed due to NH_3 gas adsorption at 0.82, 0.41, 1.58, and 3.97 eV for the Pt–$MoSe_2$, Au–$MoSe_2$, Ag–$MoSe_2$, and Pt–Au–Ag–$MoSe_2$ structures, respectively. The new peaks of DOS for doped $MoSe_2$ structures justify the modifications the bandgaps of in Fig. 4 and Table 2. The figure also demonstrates that, generally, the intensity of DOS is lower for doped $MoSe_2$ structures compared with the pristine one. Nevertheless, the DOS of pristine and doped $MoSe_2$ structures are nearly similar in spite of few dissimilarities related to the intensity as well as new energy levels mainly within the conduction band.

The new features observed in the DOS (Fig. 5) are assigned to the noble metal doping as well as adsorption of NH_3 gas. These features are allocated to quantum confinement of charge carriers as well as the hybridization between both d and s energy levels for molybdenum with selenium atoms. The electric charges are transported from both pristine and doped $MoSe_2$ structures to the NH_3 gas, where the DOS changes nearby Fermi level are moved to the p energy level of Se atom. Adsorption of NH_3 gas shifts the Fermi which specifies the hole doping for $MoSe_2$ structure. The orbital hybridization generated by NH_3 gas adsorption on the $MoSe_2$ based structures is near the Fermi level as illustrated by Fig. 5. The band structures the $MoSe_2$ based structures are almost flat demonstrating that the spin states of NH_3 gas are up nearby the Fermi level, thus, the $MoSe_2$ based structures exhibit robust adsorption energy for NH_3 gas. The occupied energy states of DOS after NH_3 gas adsorption for $MoSe_2$ based structures are the main cause of modification [42]. Subsequently, the illustrated results reveal that the noble metal doping of the $MoSe_2$ based structures improve their adsorption of NH_3 gas, with the best adsorption for the Pt–$MoSe_2$ structure.

Experimentally, S. Singh et al. demonstrated the effective utilization

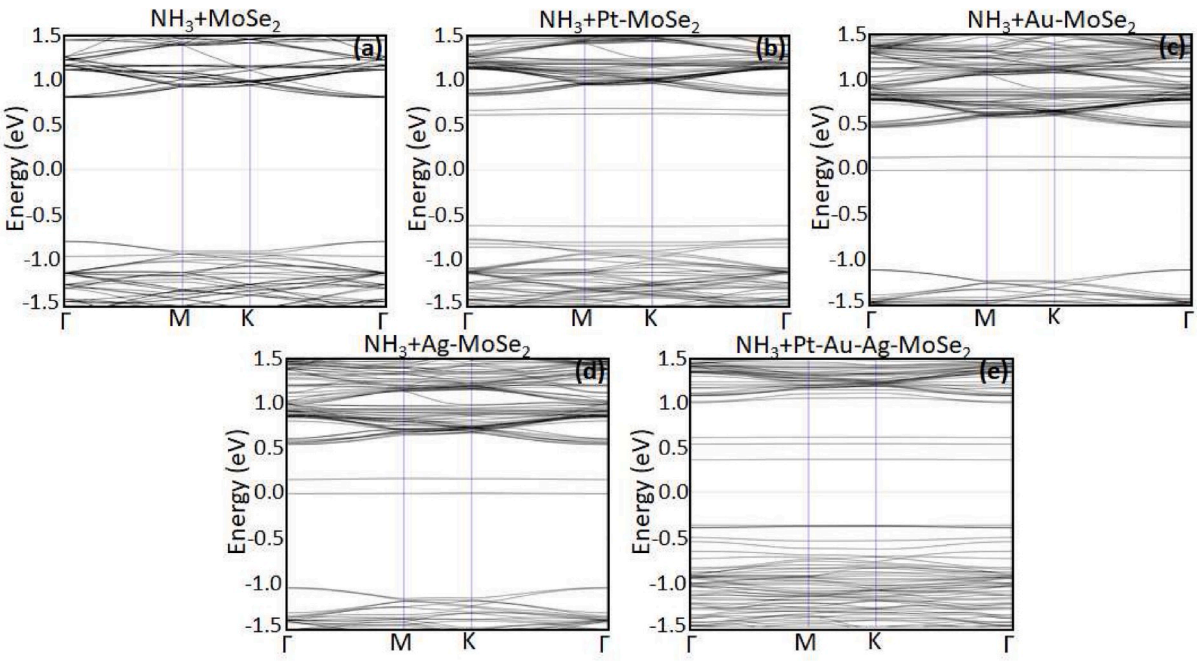

Fig. 4. Band structures of the optimized pristine and modified $MoSe_2$ structures after adsorption of NH_3 gas: a) pristine $MoSe_2$, b) Pt–$MoSe_2$, c) Au–$MoSe_2$, d) Ag–$MoSe_2$, and e) Pt–Au–Ag–$MoSe_2$.

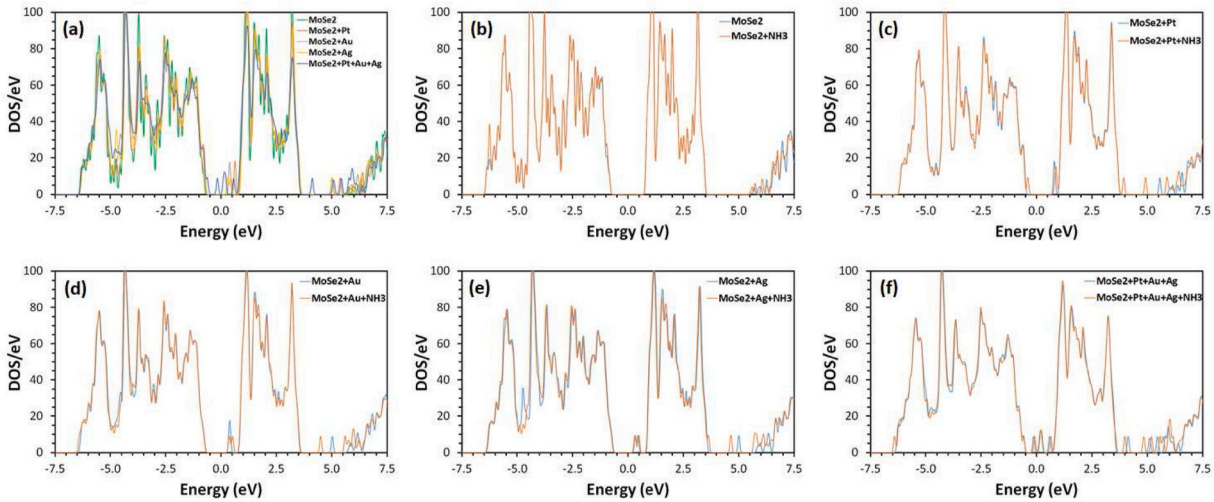

Fig. 5. Density of states (DOS) of the optimized structures: a) pristine and modified $MoSe_2$ before gas adsorption, b) pristine $MoSe_2$ before and after gas adsorption, c) Pt–$MoSe_2$ before and after gas adsorption, d) Au–$MoSe_2$ before and after gas adsorption, e) Ag–$MoSe_2$ before and after gas adsorption, and f) Pt–Au–Ag–$MoSe_2$ before and after gas adsorption.

of $MoSe_2$ nanostructure for ammonia sensor applications [11]. They demonstrated that $MoSe_2$ nanostructure can be used as a room temperature sensor for NH_3 gas with enhanced sensitivity of 10 ppm. When the sensor was exposed to NH_3 gas, its gas response measurements showed growth of resistance, indicating a p-type characteristic for the $MoSe_2$ structure. The enhanced response is assigned to electron transfer from $MoSe_2$ to NH_3 gas adsorbed, that causes decrease in hole concentration within the p-type $MoSe_2$ semiconductor hence increasing the resistance for the underlying channel of $MoSe_2$. Furthermore, the enhancement in the adsorption capacity observed for the $MoSe_2$ structures against NH_3 gas due to doping by the noble metals is mostly because of their high affinity and reactivity with NH_3 gas [43].

The response of a gas sensor (Γ) may be determined using its resistivity before and after adsorption ($\frac{1}{\sigma_b}$) and ($\frac{1}{\sigma_a}$), respectively, using [44]:

$$\Gamma = \left|\frac{\frac{1}{\sigma_a} - \frac{1}{\sigma_b}}{\sigma_b}\right|.100\% \quad (1a)$$

where σ is the electrical conductivity and can be estimated by the equation [40]:

$$\sigma = \sigma_0 e^{-\frac{E_g}{2k_B T}} \quad (2a)$$

With σ_0 is a constant that is temperature independent, E_g is the bandgap energy, T is the temperature of the $MoSe_2$ structure measured in Kelvin, and k_B is Boltzmant constant and its value is 8.62×10^{-5} eV.K^{-1}. The equations show clear enhancement of the gas response where it increases from 16% to 100% for pristine and Au–$MoSe_2$ structure, respectively. These gas response values justify the

excellent enhancement of NH_3 gas adsorption upon Au doping by a factor of 6.25 times, which supports the above DFT computations. Therefore, the noble metal doped $MoSe_2$ structures are considered sensitive elements for NH_3 gas, however, Au–$MoSe_2$ structure is the best sensitive system for NH_3 gas.

4. Conclusion

The adsorption of NH_3 gas on pristine and noble metal doped $MoSe_2$ structures has been explored using first principles computations density functional theory (DFT). The ammonia adsorption was evaluated by quantification of the adsorption energy, charge moved among NH_3 gas and the structures, adsorption energy and distance, energy band structure, along with the density of states (DOS). The adsorption characteristics of the $MoSe_2$ based structures have been greatly enhanced for NH_3 gas upon doping with noble atoms, namely: Pt, Au, Ag, and their combination. The doping produced considerable changes in the energy levels and adsorption energy. New energy bands appeared in the DOS for $MoSe_2$ structures, and their bandgaps decreased due to noble metal doping. The noble metal doped $MoSe_2$ structures exhibit improved adsorption capacity against NH_3 gas. Furthermore, noble metal doping of the $MoSe_2$ structures caused chemisorption of NH_3 gas molecule, and reduced its adsorption distances considerably. The results suggest that the best suggested structure for adsorption of NH_3 gas is Au–$MoSe_2$. The adsorption energy of NH_3 gas on Au–$MoSe_2$ structure is 3.5 times larger than that for the undoped $MoSe_2$ structure. The results of this work illustrate that the Au modified $MoSe_2$ nanostructure may be identified as a potential system for sensitive detection NH_3 gas.

Declaration of competing interest

The authors declare that they have no known competing financial interests or personal relationships that could have appeared to influence the work reported in this paper.

References

[1] M. Lashgari, M. Ghanimati, Photocatalytic degradation of H2S aqueous media using sulfide nanostructured solid-solution solar-energy-materials to produce hydrogen fuel, J. Hazard Mater. 345 (2018) 10–17.

[2] A. Bafekry, M. Faraji, M.M. Fadlallah, A. Abdolahzadeh Ziabari, A. Bagheri Khatibani, S.A.H. Feghhi, M. Ghergherehchi, D. Gogova, Adsorption of habitat and industry-relevant molecules on the MoSi2N4 monolayer, Appl. Surf. Sci. 564 (2021) 150326.

[3] S. Singh, J. Deb, U. Sarkar, S. Sharma, MoSe2 crystalline nanosheets for room-temperature ammonia sensing, ACS Appl. Nano Mater. 3 (2020) 9375–9384.

[4] S.M. Mariappan, M.K. Eswaran, U. Schwingenschlögl, T. Thangeeswari, E. Vinoth, M. Shkir, Z. Said, B. Karthikeyan, Impact of reducing agents on the ammonia sensing performance of silver decorated reduced graphene oxide: experiment and first principles calculations, Appl. Surf. Sci. 558 (2021) 149886.

[5] Y. Yong, F. Ren, Z. Zhao, R. Gao, S. Hu, Q. Zhou, Y. Kuang, Highly enhanced NH3-sensing performance of BC6N monolayer with single vacancy and Stone-Wales defects: a DFT study, Appl. Surf. Sci. 551 (2021) 149383.

[6] M. Chhowalla, H.S. Shin, G. Eda, L.-J. Li, K.P. Loh, H. Zhang, The chemistry of two-dimensional layered transition metal dichalcogenide nanosheets, Nat. Chem. 5 (2013) 263–275.

[7] S. Stankovich, D.A. Dikin, G.H. Dommett, K.M. Kohlhaas, E.J. Zimney, E.A. Stach, R.D. Piner, S.T. Nguyen, R.S. Ruoff, Graphene-based composite materials, Nature 442 (2006) 282–286.

[8] A. Bafekry, C. Nguyen, M. Obeid, M. Ghergherehchi, Modulating the electro-optical properties of doped C 3 N monolayers and graphene bilayers via mechanical strain and pressure, New J. Chem. 44 (2020) 15785–15792.

[9] A. Bafekry, M. Faraji, D. Hoat, M. Shahrokhi, M. Fadlallah, F. Shojaei, S. Feghhi, M. Ghergherehchi, D. Gogova, MoSi2N4 single-layer: a novel two-dimensional material with outstanding mechanical, thermal, electronic and optical properties, J. Phys. Appl. Phys. 54 (2021) 155303.

[10] A. Bafekry, F. Shojaei, M.M. Obeid, M. Ghergherehchi, C. Nguyen, M. Oskouian, Two-dimensional silicon bismotide (SiBi) monolayer with a honeycomb-like lattice: first-principles study of tuning the electronic properties, RSC Adv. 10 (2020) 31894–31900.

[11] S. Singh, R.C. Singh, S. Sharma, Room temperature ammonia sensing using MoSe2 nanostructures, Mater. Today Proc. 28 (2020) 11–13.

[12] Z. Xiao, W. Wu, X. Wu, Y. Zhang, Adsorption of NO2 on monolayer MoS2 doped with Fe, Co, and Ni, Cu: a computational investigation, Chem. Phys. Lett. 755 (2020) 137768.

[13] J. Wang, Q. Zhou, L. Xu, X. Gao, W. Zeng, Gas sensing mechanism of dissolved gases in transformer oil on Ag–MoS2 monolayer: a DFT study, Phys. E Low-dimens. Syst. Nanostruct. 118 (2020) 113947.

[14] S. Tongay, J. Zhou, C. Ataca, K. Lo, T.S. Matthews, J. Li, J.C. Grossman, J. Wu, Thermally driven crossover from indirect toward direct bandgap in 2D semiconductors: MoSe2 versus MoS2, Nano Lett. 12 (2012) 5576–5580.

[15] G. Jeevanandham, K. Vediappan, Z.A. ALOthman, T. Altalhi, A.K. Sundramoorthy, Fabrication of 2D-MoSe2 incorporated NiO Nanorods modified electrode for selective detection of glucose in serum samples, Sci. Rep. 11 (2021) 1–13.

[16] D. Zhang, Q. Li, P. Li, M. Pang, Y. Luo, Fabrication of Pd-decorated MoSe2 nanoflowers and density functional theory simulation toward ammonia sensing, IEEE Electron. Device Lett. 40 (2019) 616–619.

[17] E. Salih, A.I. Ayesh, First principle Study of transition metals codoped MoS2 as a gas sensor for the detection of NO and NO2 gases, Phys. E Low-dimens. Syst. Nanostruct. (2021) 114736.

[18] J. Ge, L. Fan, J. Wang, Q. Zhang, Z. Liu, E. Zhang, Q. Liu, X. Yu, B. Lu, MoSe2/N-doped carbon as anodes for potassium-ion batteries, Adv. Energy Mater. 8 (2018) 1801477.

[19] S.Y. Choi, Y. Kim, H.-S. Chung, A.R. Kim, J.-D. Kwon, J. Park, Y.L. Kim, S.-H. Kwon, M.G. Hahm, B. Cho, Effect of Nb doping on chemical sensing performance of two-dimensional layered MoSe2, ACS Appl. Mater. Interfaces 9 (2017) 3817–3823.

[20] D. Zhang, Z. Yang, P. Li, M. Pang, Q. Xue, Flexible self-powered high-performance ammonia sensor based on Au-decorated MoSe2 nanoflowers driven by single layer MoS2-flake piezoelectric nanogenerator, Nano Energy 65 (2019) 103974.

[21] H. Luo, Y. Cao, J. Zhou, J. Feng, J. Cao, H. Guo, Adsorption of NO2, NH3 on monolayer MoS2 doped with Al, Si, and P: a first-principles study, Chem. Phys. Lett. 643 (2016) 27–33.

[22] E. Salih, A.I. Ayesh, DFT investigation of H2S adsorption on graphenenanosheets and nanoribbons: comparative study, Superlattice. Microst. 146 (2020) 106650.

[23] E. Salih, A.I. Ayesh, Enhancing the sensing performance of zigzag graphene nanoribbon to detect NO, NO2, and NH3 gases, Sensors 20 (2020) 3932.

[24] E. Salih, A.I. Ayesh, Computational study of metal doped graphene nanoribbon as a potential platform for detection of H2S, Mater. Today Commun. 26 (2021) 101823.

[25] B. Salah, A.I. Ayesh, Fabrication of H2S sensitive gas sensors formed of SnO2-Fe2O3 composite nanoparticles, Mater. Chem. Phys. (2021) 124597.

[26] E. Salih, A.I. Ayesh, Sensitive SO2 gas sensor utilizing Pt-doped graphene nanoribbon: first principles investigation, Mater. Chem. Phys. 267 (2021) 124695.

[27] J.P. Perdew, K. Burke, M. Ernzerhof, Generalized gradient approximation made simple, Phys. Rev. Lett. 77 (1996) 3865.

[28] S. Grimme, Semiempirical GGA-type density functional constructed with a long-range dispersion correction, J. Comput. Chem. 27 (2006) 1787–1799.

[29] E. Salih, A.I. Ayesh, Pt-doped armchair graphene nanoribbon as a promising gas sensor for CO and CO2: DFT study, Phys. E Low-dimens. Syst. Nanostruct. 125 (2021) 114418.

[30] D. Liu, Y. Gui, C. Ji, C. Tang, Q. Zhou, J. Li, X. Zhang, Adsorption of SF6 decomposition components over Pd (1 1 1): a density functional theory study, Appl. Surf. Sci. 465 (2019) 172–179.

[31] E. Salih, A.I. Ayesh, CO, CO2, and SO2 detection based on functionalized graphene nanoribbons: first principles study, Phys. E Low-dimens. Syst. Nanostruct. (2020) 114220.

[32] E. Salih, A.I. Ayesh, First principle investigation of H2Se, H2Te and PH3 sensing based on graphene oxide, Phys. Lett. 384 (2020) 126775.

[33] R.S. Mulliken, Electronic population analysis on LCAO–MO molecular wave functions. I, J. Chem. Phys. 23 (1955) 1833–1840.

[34] Y. Zhang, T.-R. Chang, B. Zhou, Y.-T. Cui, H. Yan, Z. Liu, F. Schmitt, J. Lee, R. Moore, Y. Chen, Direct observation of the transition from indirect to direct bandgap in atomically thin epitaxial MoSe 2, Nat. Nanotechnol. 9 (2014) 111.

[35] V. Nagarajan, R. Chandiramouli, MoSe2 nanosheets for detection of methanol and ethanol vapors: a DFT study, J. Mol. Graph. Model. 81 (2018) 97–105.

[36] V.E.C. Padilla, M.T.R. de la Cruz, Y.E.Á. Alvarado, R.G. Díaz, C.E.R. García, G. H. Cocoletzi, Studies of hydrogen sulfide and ammonia adsorption on P-and Si-doped graphene: density functional theory calculations, J. Mol. Model. 25 (2019) 94.

[37] T. Pakornchote, A. Ektarawong, B. Alling, U. Pinsook, S. Tancharakorn, W. Busayaporn, T. Bovornratanaraks, Phase stabilities and vibrational analysis of hydrogenated diamondized bilayer graphenes: a first principles investigation, Carbon 146 (2019) 468–475.

[38] M.G. Ahangari, A.H. Mashhadzadeh, M. Fathalian, A. Dadrasi, Y. Rostamiyan, A. Mallahi, Effect of various defects on mechanical and electronic properties of zinc-oxide graphene-like structure: a DFT study, Vacuum 165 (2019) 26–34.

[39] X. Gao, Q. Zhou, J. Wang, L. Xu, W. Zeng, Adsorption of SO2 Molecule on Ni-Doped and Pd-Doped Graphene Based on First-Principle Study, Applied Surface Science, 2020, p. 146180.

[40] T. Liu, Z. Cui, X. Li, H. Cui, Y. Liu, Al-doped MoSe2 monolayer as a promising biosensor for exhaled breath analysis: a DFT study, ACS Omega 6 (2020) 988–995.

[41] S. Ma, L. Su, L. Jin, J. Su, Y. Jin, A first-principles insight into Pd-doped MoSe2 monolayer: a toxic gas scavenger, Phys. Lett. 383 (2019) 125868.

[42] G.K. Walia, D.K.K. Randhawa, First-principles investigation on defect-induced silicene nanoribbons—a superior media for sensing NH3, NO2 and NO gas molecules, Surf. Sci. 670 (2018) 33–43.
[43] W. Hui, G. Chang, W. Gao, Exploring the electronic and magnetic properties of noble metal (Pd, Pt, Au) adsorbed MoSe2 monolayers and their performance towards sensing gas molecules, Phys. E Low-dimens. Syst. Nanostruct. 122 (2020) 114167.
[44] A.I. Ayesh, A.A. Alyafei, R.S. Anjum, R.M. Mohamed, M.B. Abuharb, B. Salah, M. El-Muraikhi, Production of sensitive gas sensors using CuO/SnO 2 nanoparticles, Appl. Phys. A 125 (2019) 1–8.